

Predicting the Electrical Behavior of Colored Photovoltaic Modules Integrating Absorptive or Diffusive Layers or PMMA Films Doped with Organic Chromophores

Martina Pelle,* Irene Motta, Gabriella Gonnella, Alessio Dessì, Lidia Armelao, Gregorio Bottaro,* Massimo Calamante,* Alessandro Mordini, and David Moser

The advancement of photovoltaic (PV) technology is critical for sustainable energy production, with silicon-based solar cells being the most prevalent due to their efficiency and cost-effectiveness. In recent years, the use of materials to change the color of conventional silicon-based PV cells, materials that can be laminated or not during the construction of the PV module, has become widespread. Colored PV cells offer aesthetic versatility, making them suitable for integrated architectural applications. However, these materials affect the performance of the final product. This study focuses on developing a predictive model for the performance of colored silicon PV cells. A comprehensive approach combining experimental data and computational simulations is employed to understand the impact of various colors on the electrical performance of colored PV modules, based on the optical properties of the colored layers. The model demonstrates high accuracy across a range of coloring technologies, including selective absorbers, diffusive layers, and fluorescent materials. The developed model accurately predicts the performance metrics of colored PV cells, providing valuable insights for optimizing design and material selection.

the use of photovoltaic (PV) technology is essential^[1] In recent decades, there has been a rapid expansion of installed PV, recently reaching a value of 1 TW,^[2] and further development is expected in the coming years.^[3] In particular, the expected future development will be granular, meaning low-power installations widely distributed across the territory rather than large PV fields. This approach uses energy in the same place where it is produced, reducing distribution costs.^[4,5] This will require the integration of PV panels into the built environment, which can be challenging due to the black or dark blue coloration of silicon-based PV devices. This might be perceived as unsightly by users and architects since the standard appearance of PV modules might overload the architectural characteristics of buildings, especially in the existing built environment.^[6–10]

Additionally, as in the case of European

Member States, utilizing building surfaces for solar energy harvesting can contribute to reach the targets of renewable energy in the energy mix while lowering the requirement for land to be set aside for solar farms.^[11] To address this issue, it is possible to either use PV cells as a basic element for the design of patterns or incorporate a colored and transparent material to conceal the true color of the device.^[12–15] The development of modules that

1. Introduction

With the aim of countering climate change caused by the accumulation of greenhouse gases, human society is evaluating new strategies to undertake a fast and effective energy transition from fossil fuels to renewable sources. To limit the increase of temperatures to below 2 °C, as stipulated by the Paris Agreement,

M. Pelle, G. Gonnella, D. Moser
Institute for Renewable Energy
Eurac Research
Via Alessandro Volta 13/a, 39100 Bolzano, Italy
E-mail: Martina.Pelle@eurac.edu


I. Motta, L. Armelao
Dipartimento di Scienze Chimiche and INSTM
Università di Padova
via Marzolo 1, I-35131 Padova, Italy

A. Dessì, M. Calamante, A. Mordini
Institute of Chemistry of Organometallic Compounds (CNR-ICCOM)
National Research Council
50019 Sesto Fiorentino (FI), Italy
E-mail: mcalamante@iccom.cnr.it

L. Armelao
Dipartimento di Scienze Chimiche e Tecnologie dei Materiali (DSCTM)
Consiglio Nazionale delle Ricerche
Piazzale A. Moro 7, 00185 Roma, Italy

G. Bottaro
CNR ICMATE and INSTM, Dipartimento di Scienze Chimiche
Università di Padova
via Marzolo 1, I-35131 Padova, Italy
E-mail: gregorio.bottaro@cnr.it

M. Calamante, A. Mordini
Department of Chemistry “Ugo Schiff”
University of Florence
via della Lastruccia 13, 50019 Sesto Fiorentino, Italy

 The ORCID identification number(s) for the author(s) of this article can be found under <https://doi.org/10.1002/solr.202400570>.

DOI: 10.1002/solr.202400570

may conceal the PV cells beneath colored patterns, which limits the perception of the actual material of the cells, has significantly impacted the aesthetic acceptability of building-integrated PVs (BIPV) applications, improving the visual rendering of PV modules, required for broader architectural application. The modification of the visual rendering of a PV module can be obtained by means of absorptive materials,^[16–18] by using nanostructures leveraging interference effects^[19–21] or implementing optical filters.^[22,23] Nonetheless, modifying the color rendering of a PV material influences also the electric performance of the device since the reflected portion of the electromagnetic spectrum needed to perceive the desired color is subtracted to the power conversion mechanism of the PV device.^[12,24–27] Furthermore, introducing colored features in PV determines an increase in the cost, which is due to 1) the introduction of colored layers, which alters the standard manufacturing process of an uncolored product; and 2) a reduction in the energy yield of the BIPV module, which impacts the economic profitability of the installation.^[28] Therefore, personalization makes it difficult to accurately evaluate the overall technical performance of these products, whereby aesthetic and energy considerations must be balanced. Hence, there is a need to raise awareness about colored BIPV technologies in terms of the electrical behavior of a wide range of colored modules, reliably assessing the influence of color on their power generation. Up to now, the main driver for colored modules development has been the sole aesthetic, while less focus has been devoted to the optimization of the modules' performance and appearance at the same time.

In this context, a tool allowing to predict the electrical performance and color rendering of the final product based on the optical and electrical characteristics of its single components could be very useful in saving time and resources usually invested in prototype development. This modeling approach provides high degree of precision and flexibility in considering different coloring techniques and PV technologies and might provide useful information for performance optimization of the final device.^[28] Therefore, the present work introduces a modeling framework to predict the short-circuit current (I_{SC}) spectral response (SR) and the integrated I_{SC} value of colored PV modules, based on the optical properties of the involved layers. These modules can have either a two- or three-layer structure, featuring a monocrystalline silicon solar cell as the bottom layer and a colored top layer. The model utilizes the SR of the PV cell and the spectral optical properties of the colored layers as input parameters.

The model has been applied and validated for colored components which behave as 1) selectively absorptive layers, 2) diffusive layers, or 3) absorptive layers with fluorescent characteristics. The latter have been analyzed due to their potential ability to compensate for efficiency losses caused to color rendering. The following discussion will first define the structure of the examined device under test (DUT) and address the choice of the materials used to simulate the different coloring layer technologies. Experimental data on the electrical performance and the colorimetric characteristics of the DUT have been measured by means of a custom experimental setup, which is described later in detail. Next, the modeling strategy is explained by defining how input data are combined to yield the calculated

output I_{SC} spectra and the integrated I_{SC} of the DUT. The results of the study are presented by type of employed coloring layer, accompanied by the characterization of their photophysical properties, as transmittance spectra and emission parameters for the fluorescent films. The comparison between experimental and calculated DUT electrical performance data is reported and used to assess the accuracy of the predictive model.

2. General Methodology

2.1. DUT Structure

The basic components of colored commercial modules' stacks are a back sheet, a PV active layer, an encapsulant, and a protective front glass cover. The color of the overall device can be modified by working on the encapsulant or the front glass, or by introducing colored interlayers in the described system.^[14] Hence, a colored commercial PV cell has a complicated multi-layer structure (**Figure 1a**) that is not straightforward to reproduce in a laboratory. In many cases, they are protected by patents so that the composition of the different layers and details of the production process are not available. For this reason, the development of a predictive model capable of determining the performance of the colored module starting from the optical properties of the different layers (transmittance and reflectance spectra, refractive index spectra) is a demanding task.

In this framework, we decided to start our investigation by building a simplified version of a colored PV module consisting of a monocrystalline Si PV cell and a colored layer on top of it (**Figure 1b**). In this way, both the single layers and the final DUT can be studied.

We considered three types of colored materials characterized by different morphological and optical properties (**Figure 1c**), namely, 1) optical filters made of Schott colored glass, 2) commercial ground glass diffusers to simulate a white layer, and 3) colored and strongly fluorescent polymeric thin films synthesized by us.

The choice of materials for the colored layer reflects an increase in complexity of the studied DUT. The employed optical filters are scatter-free glass slates with optically polished faces, so their coloration is due only to selective absorption of portions of the visible spectrum. Therefore, they provide the simplest way to introduce a colored layer. Conversely, ground glass diffusers feature a sandblasted surface with variable grit, providing a range of scattering effects from fine to coarse. They act as light scattering elements that can be used to give a white hue to the DUT, particularly sought-after for colored PV modules. This is an example of a material in which coloration is achieved by modification of its morphology, rather than its composition. Finally, polymeric fluorescent films provide a different approach both for their geometry (interlayer thin sheets rather than thick cover glass) (**Figure 1b**) and light management. Here, the film's coloration is determined by the absorption properties of the embedded dye. This dye, being strongly fluorescent, behaves as a secondary light source. In this way, a portion of the absorbed photons is re-emitted and can reach the PV layer. This type of approach has

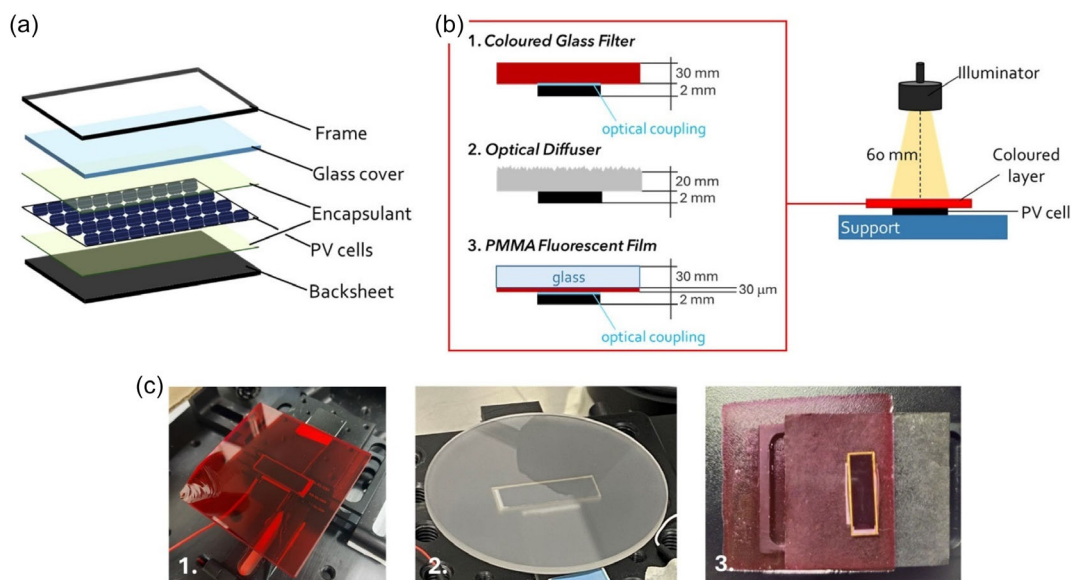


Figure 1. a) Simplified schematics of the basic components in a commercial PV module. b) List of the DUT configurations used with the different examined colored layers and placement of the DUT in the experimental setup with respect to the light source. c) Digital photographs of one representative sample for each examined colored layer technology.

already been proposed for use in solar cells to enhance the SR in the high-energy region of the solar spectrum, leading to an increase in the photocurrent produced by the PV cell.^[29,30] The behavior of the Si PV cell under monochromatic light source has been investigated by placing the colored layer directly on top of the cell. The DUT has been successively improved by introducing optical coupling between the PV cell and the colored layer using a microscopy immersion oil.

2.2. Experimental Setup

To acquire the experimental data used to develop and validate the predictive model for the I_{SC} spectra and the integrated I_{SC} , we built an experimental setup around a research grade spectrofluorometer (**Figure 2a**) that has been used as a highly versatile light source, providing a light output that can be tailored both spectrally and spatially (see Experimental Section for further

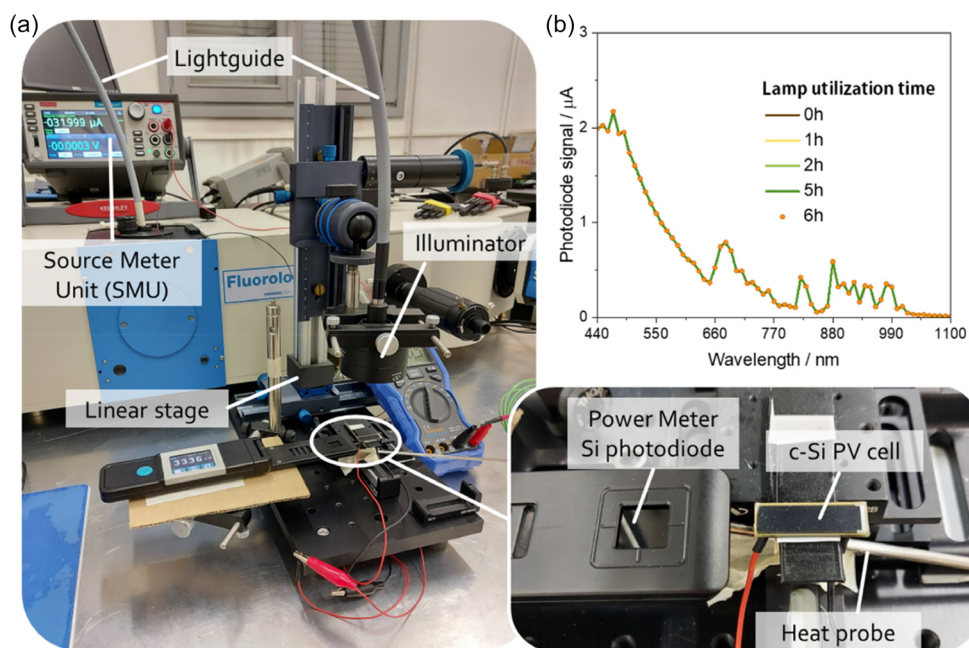


Figure 2. a) Experimental setup for the collection of electrical input data. b) Lamp intensity monitored with spectrofluorometer internal photodiode, evidencing the high stability of the illumination system.

details).^[31] A monocrystalline, single-module Si PV cell with active area of $2.2 \times 0.7 \text{ cm}^2$ has been chosen as test PV cell to be integrated in the DUT.

The 450 W Xe arc lamp of the spectrofluorometer was used as monochromatic light source. The PV cell was illuminated employing a vis/NIR transmitting optical fiber coupled with an uncoated UV fused silica plano-convex lens to collimate the beam over a circular area of 50 mm diameter. The stability of the lamp was monitored through a spectrofluorometer internal photodiode which measured the intensity of the light before entering the lightguide. The photodiode output was monitored over 6 h, observing signal fluctuations lower than 1% (Figure 2b). The illuminator was mounted on a xyz linear stage, allowing alignment of the illumination spot over the PV cell. Minimum steps along the directions of the stage were 1 mm for x and y , and 0.25 mm for z . The distance between the illuminator and the PV cell surface was set at 60 mm. The optical power of the incident beam was measured through a calibrated Si photodiode. I_{SC} SRs under monochromatic light were acquired by means of a source meter unit (SMU) synchronized with the

spectrofluorometer. Repeatability of data measured with the described setup was ensured by performing a series of acquisitions of the bare PV cell I_{SC} and of the incident optical power spectra under constant illumination conditions (Figure S1, Supporting Information). Measurements show negligible variation over the whole investigated spectral range (440–1100 nm), confirming the reliability of the designed setup.

The ability of the colored filters to change the aesthetic appearance of the bare PV was evaluated via colorimetric tests on the samples, by using a vertical colorimeter (see Experimental Section for further details). The CIE Lab coordinates of the analyzed DUT are reported in Table S3, Supporting Information (bare PV cell) and Table S4–S6, Supporting Information (colored DUT). The color of the analyzed DUT has been represented in the CIE Lab color space, as shown in Figure S1 (Supporting Information). Based on the color coordinates, the difference in color (ΔE) between the bare PV and the DUT has been calculated according to the CIE 2000 formula, after proper transformation of the CIE Lab coordinates in CIE LCH coordinates, as:^[32]

$$\Delta E_{00} = \sqrt{\left(\frac{\Delta L'}{k_L S_L}\right)^2 + \left(\frac{\Delta C'}{k_C S_C}\right)^2 + \left(\frac{\Delta H'}{k_H S_H}\right)^2 + R_T \left(\frac{\Delta C'}{k_C S_C}\right) \left(\frac{\Delta H'}{k_H S_H}\right)} \quad [-] \quad (1)$$

where $\Delta L'$ is the difference in lightness between the two colors, $\Delta C'$ is the difference in the chroma, and $\Delta H'$ is the difference in the color hue. k_L , k_C , and k_H are parametric factors and S_L , S_C , and S_H are weighting functions that adjust the total color difference to include the characteristics of the nonuniform color discrimination threshold of the human eye. R_T is a rotation function that is applied to weighted hue and chroma differences. The color difference has been calculated under reference conditions, with the parametric factors set equal to $k_L = k_C = k_H = 1$. According to the standard, slight differences in two colors would only be detectable by the human eye upon close observation if their color difference is $\Delta E < 2$. If the color difference is $\Delta E > 2$, the human eye can easily perceive the two color as distinct. Therefore, this parameter can provide a valuable indication of the ability of the colored layers to modify the aesthetic appearance of the colored DUT.

2.3. Modeling Strategy

2.3.1. Bare PV Device Electrical Properties

Based on the measured data of the current generated by the test cell and the power of the source, the external quantum efficiency (EQE_{PV}) and the SR of the bare PV cell were calculated as follows:

$$EQE_{PV}(\lambda) = \left(\left(\frac{I_{sc,mis}(\lambda)}{P_{source}(\lambda) * \lambda} \right) * 100 * \frac{hc}{q} \right) [\%] \quad (2)$$

$$SR_{PV}(\lambda) = \frac{EQE_{PV}(\lambda)}{100 * \frac{hc}{q}} * \lambda [-] \quad (3)$$

where P_{source} is the measured power of the light source; $I_{sc,mis}$ is the current generated by the test cell, illuminated by the source,

measured using a digital multimeter; λ is the wavelength expressed in nm; q is the elementary charge of an electron expressed in coulombs; h is the Planck's constant expressed in $\text{m}^2 \text{kg s}^{-1}$; and c is the speed of light expressed in m s^{-1} .

These data were used to simulate the spectral current generated by the bare cell by multiplying the light source spectrum $E_o(\lambda) = P_{source}$ by the SR of the cell $SR_{PV}(\lambda)$, as follows:

$$I_\lambda = E_o(\lambda) \cdot SR_{PV}(\lambda) [A] \quad (4)$$

2.3.2. Electrical Response of the Colored Device

The developed model aims at predicting the effects of a colored layer on the electrical output of a Si PV cell. The optical characteristics of the different elements involved are taken as input data for the model. The spectral transmittances obtained from the spectrophotometric measurements were used to calculate the equivalent irradiance spectrum Φ_λ , which reaches the PV cell in the colored DUT configuration. To obtain the equivalent irradiance spectrum Φ_λ , the spectral transmittance of the colored layer $\tau(\lambda)$ is multiplied by the light source spectrum $E_o(\lambda)$, as follows:

$$\Phi_\lambda = E_o(\lambda) \cdot \tau(\lambda) [W] \quad (5)$$

In this way, it is possible to associate each spectral transmittance with a color and the electrical output of the corresponding DUT. By combining the equivalent spectrum Φ_λ and the SR of the c-Si cells, it is possible to calculate the spectral current produced by the colored DUT:

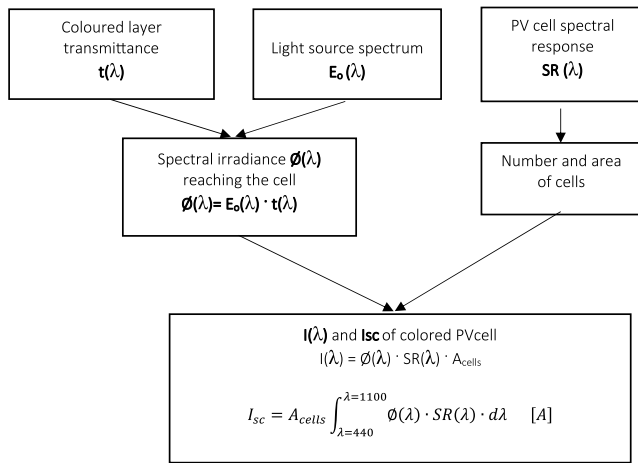


Figure 3. Scheme of the modeling approach structure for the DUT including colored layer.

$$I_{\lambda} = \Phi(\lambda) \cdot SR_{PV}(\lambda) [A] \quad (6)$$

By integrating this product over the response range of the PV cell, the current density generated by the device is obtained. The short-circuit current is then obtained by multiplying by the active area of the device. A schematic overview of the modeling approach for the colored DUT is reported in **Figure 3**.

2.3.3. Optical Coupling Between the DUT Components

A commercial PV module consists of a multilayer structure, where the different components are first layered and then undergo a thermal and mechanical process, called lamination, needed to couple all the layers together and guarantee the safety and reliability of the final device. The lamination process determines the optical coupling between each adjacent component of the stack, and it modifies the optical characteristics of the device. A correction to the model has been therefore implemented, by improving the modeling of the optical behavior of the module's layers once they are coupled during the modules' lamination process. In fact, in a commercial module, the used encapsulant materials (usually polyvinyl butyral (PVB) or ethylene-vinyl acetate (EVA)) have a refractive index very similar to the one of the front glass ($n_{EVA} \approx n_{glass} \approx 1.5$), and thus the reflectivity at the interface between these two elements is very low or completely absent if compared to the reflectivity at the interface between the glass and the air ($n_{air} \approx 1$). Therefore, the total transmittance of the encapsulated components increases. Since predicting the electrical behavior of a colored device requires the characterization of the optical properties of the layers in front of the PV cell, the proposed model includes the possibility to model the properties of the optically coupled layers.

To account for this behavior, Stokes's equations have been used to retrieve the complex refractive index of each component of the DUT from the measured optical properties in air, under the hypothesis of symmetric behavior of the components. The detailed deduction process for the optical coupling is available in the Supporting Information.

3. Results and Discussion

3.1. Bare PV Cell Characterization: SR, EQE and Simulated Short-Circuit Current (I_{sc})

The objective of this study was to develop a model capable of accurately predicting the behavior of a PV cell under illumination, with a particular focus on its response to the application of a film that altered its coloration. Specifically, we aimed to assess the model's predictive accuracy concerning the cell's performance at wavelengths that were either absorbed or scattered by the film applied to its surface. We sought to determine the model's efficacy in forecasting the current generated at these specific wavelengths. To achieve this, we first constructed a model of the cell's current output, incorporating both its SR and the intensity of incident light across varying wavelengths. This approach allowed us to simulate the cell's response more precisely as a function of the incident wavelength and to evaluate the effect of the altered coloration on its energy conversion efficiency. **Figure 4** reports the EQE and SR of the PV device under investigation, calculated from the measurement, as described in Section 2.3.1.

3.2. Colored Filters and Diffusive Glass

The model has been applied on a prototype system, including the PV cell coupled to the colored and diffusive glass layers described in Section 2. **Figure 5** reports the result of the measured (exp.) and the simulated (calc.) SR in current of the analyzed DUT. In the chart are also reported the measured spectral transmittance of the filters and the calculated relative percentage squared error (SE) of the simulated PV device response. **Table 1** reports the measured and simulated short-circuit currents of the devices, as well as their relative percentage SE. Data calculated by the model show a good agreement with experimental measured data, with a SE on the final I_{sc} lower than 1% for all the analyzed configurations (**Figure 6**), and always lower than 2% when calculated for the spectrally resolved response (**Figure 5**).

The ability of the colored filters to change the aesthetic appearance of the bare PV was evaluated via colorimetric tests on the

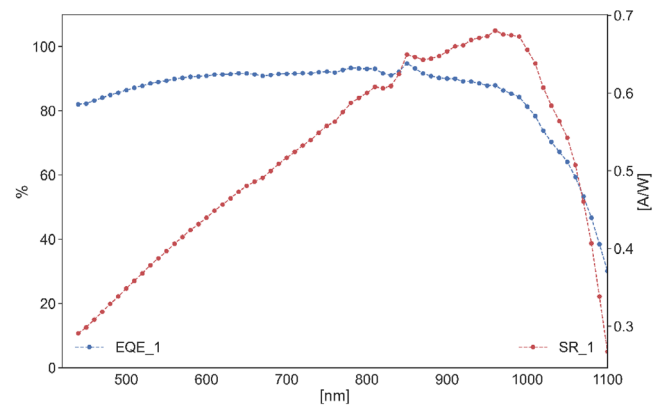


Figure 4. EQE (blue dot line) and SR (red dot line) calculated based on the measured current generated by the cell and spectral power of the light source.

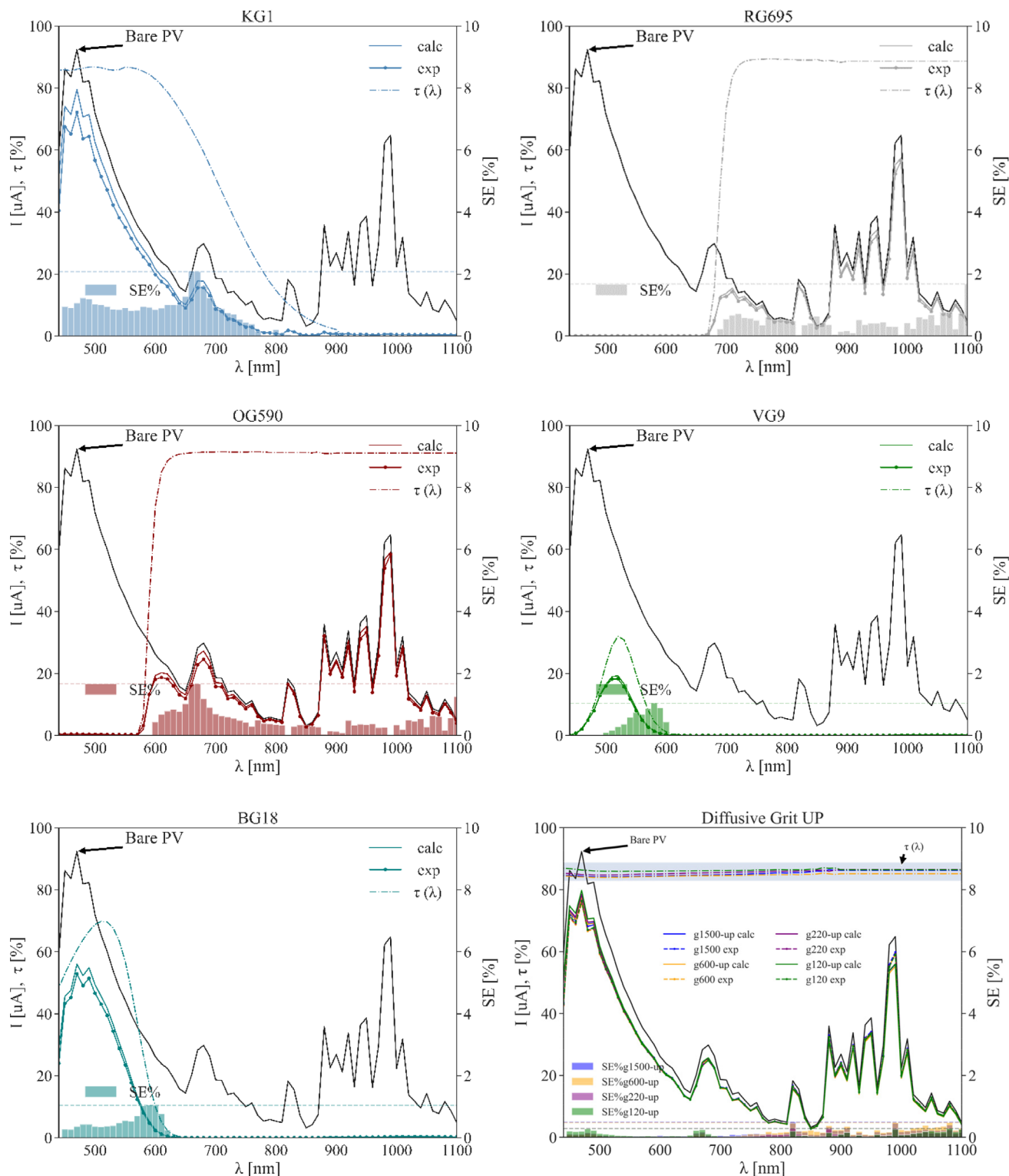


Figure 5. Result of the measured (exp.) and the simulated (calc.) SR in current of the analyzed systems, reported on top of each chart. The charts also report the measured spectral transmittance $\tau(\lambda)$ of the filters and the calculated spectral SE in percentage (SE%) of the simulated PV devices response.

Table 1. Measured and simulated short-circuit currents of the devices, relative percentage SE of the I_{SC} of the analyzed DUT.

	I_{SC} calc. [mA]	I_{SC} exp. [mA]	SE%
BG18	5.65	5.36	0.31
VG9	1.32	1.29	0.05
OG590	8.84	8.39	0.28
RG695	6.64	6.32	0.26
KG1	10.43	9.54	0.88
g1500-up	16.38	16.61	0.020
g600-up	16.28	16.36	0.002
g220-up	16.47	16.39	0.003
g120-up	16.62	16.39	0.020

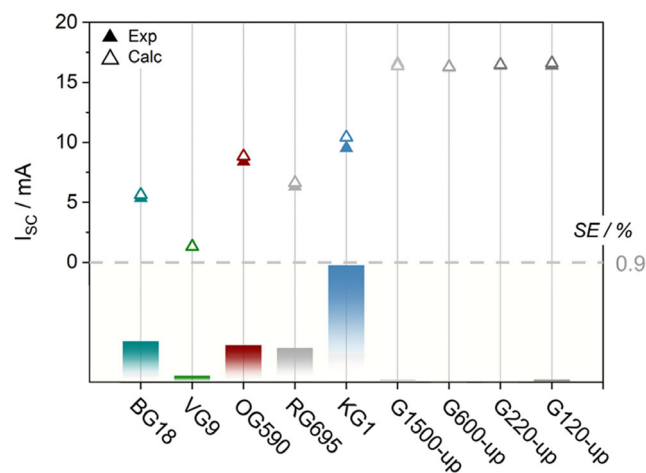


Figure 6. Experimental and calculated I_{SC} values for the colored filters and the diffusers. The SE% for each pair of exp.–calc. values is displayed as a column plot, with notable mark displayed on the furthest right axis.

samples, by using a vertical colorimeter. The evaluation was performed by calculating the difference in color (ΔE_{00}) between the bare PV and the samples. Preliminary results highlight that the KG1 sample shows the stronger potential to change the color of the device while reducing the short circuit current by about 37% when compared to the electrical response of the bare cell PV. The lowest reduction is shown by the RG690 sample, which has also the lower color difference (Figure 7).

3.3. Fluorescent Polymeric Films

Fluorescent polymer films were prepared by dispersing organic fluorophores into polymethyl methacrylate (PMMA). Specifically, they were prepared using the drop-casting procedure starting from chloroform solutions of the fluorophore and PMMA in different weight ratios, according to the previously published procedure.^[33,34] Briefly, a solution containing 60 mg of PMMA and the appropriate amount of fluorophore to reach concentrations ranging from 0.4% to 2.0% was poured onto a $50 \times 50 \times 3 \text{ mm}^3$

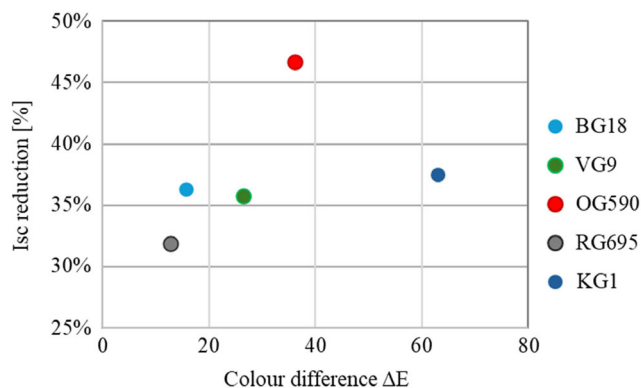


Figure 7. Colorimetric characterization (color difference) and I_{SC} reduction of the DUT with colored filters, compared to the bare PV cell.

optically pure glass substrate (Edmund Optics Ltd. BOROFLOAT window 50×50 TS). The product was obtained after evaporation at room temperature in a closed environment. The fluorophores used for the preparation of the films include Lumogen F Red 350 (BASF) (LR305), a commercial perylene diimide dye, and the new quinoxaline fluorophore DQ-Th2. DQ-Th2 belongs to a series of fluorophores with a donor–acceptor–donor structure recently developed by us for applications in the field of luminescent solar concentrators (LSCs). The synthetic procedures and spectroscopic characterization of these fluorophores have recently been published.^[34] Validation analysis of the model has been carried out for all DQ-Th fluorophores, but given the analogous properties, we report and comment for brevity only the data related to DQ-Th2 (the graphs with transmittance of the molecules, experimental and calculated electrical data for all the other dyes in the DQ-Th series are reported in Figure S2–S6, Supporting Information). The two fluorophores showed different properties: LR305 represents the state-of-the-art for fluorophores used in LSCs due to its high fluorescence quantum yield ϕ , molar attenuation coefficient ϵ , and absorption at the peak intensity of solar radiation^[35] (Figure 8 and Table 2). DQ-Th2 has a maximum absorption wavelength similar to that of LR305, but with a lower ϵ and ϕ . However, DQ-Th2 exhibits a higher Stokes shift, which reduces self-absorption effects within the PMMA polymer matrix.^[36]

Similar to what has been reported in the previous section, here the results regarding the fluorescent polymeric films are presented. Figure 9 and 10 report the results of the measured (exp.) and the simulated (calc.) SR in current for the configurations integrating the DQ-Th2 and the LR305 films, respectively. The figures also report the measured spectral transmittance of the films at different concentrations and the calculated spectral SE of the simulated PV device response. The trend of the SR of the DUT with rising dye concentration is accurately replicated by the simulations. The model's precision in forecasting the electrical behavior within the dye absorption region highlights a decrease, especially for LR305. However, the SEs evaluated on the generated short circuit current show that the model is reliable (Table 3).

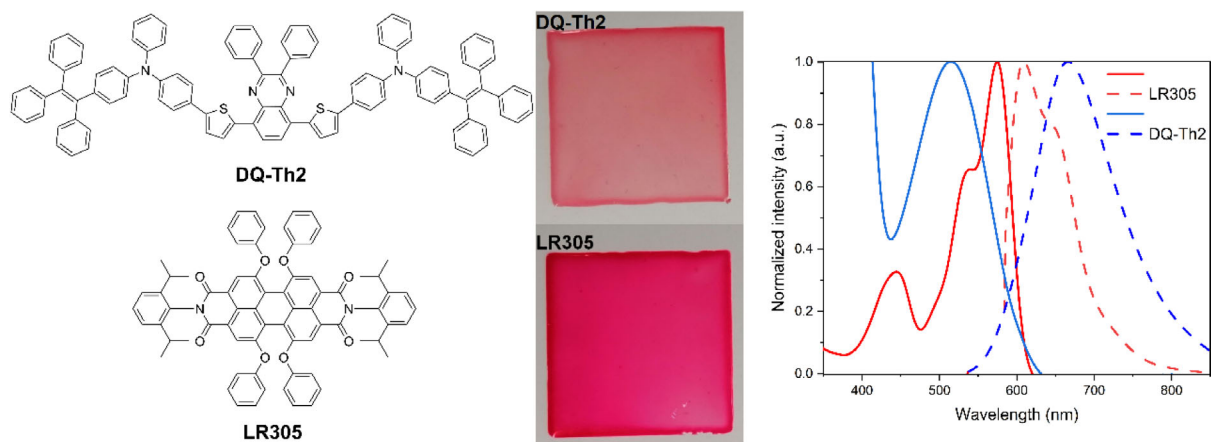


Figure 8. Chemical structure of fluorescent organic compounds DQ-Th2 and LR305, PMMA film prepared with them, and the absorption spectra (solid line) and emission spectra (dashed line) of the films prepared with the two fluorophores (concentration 0.4 wt%).

Table 2. Spectroscopical data of LR305 and DQ-Th2 in toluene and PMMA films.

	Toluene solutions				PMMA films (0.4%)		
	ϵ [$M^{-1} cm^{-1}$]	λ_{max}^{abs} [nm]	λ_{max}^{emi} [nm]	ϕ	λ_{max}^{abs} [nm]	λ_{max}^{emi} [nm]	ϕ
LR305	48 000	574	604	0.99	575	609	0.85
DQ-Th2	27 400	517	644	0.57	517	666	0.65

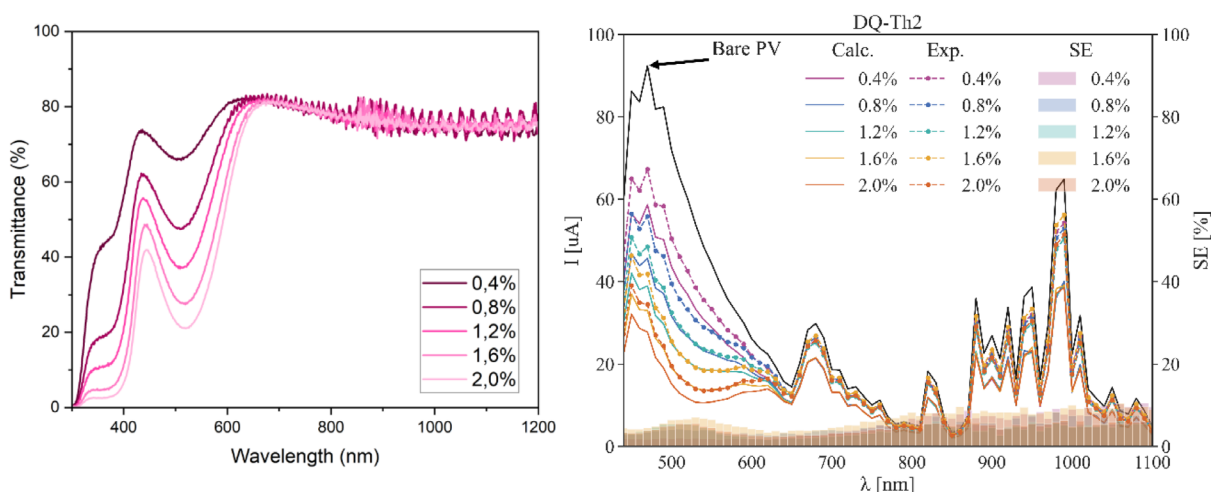


Figure 9. Result of the measured (exp.) and the simulated (calc.) SR in current of the analyzed system integrating DQ-Th2 film (on the left). The chart also reports the calculated spectral SE in percentage (SE%) of the simulated PV devices response. The measured spectral transmittance $\tau(\lambda)$ of the filters at different concentrations is reported in the chart on the right.

3.3.1. Optical Coupling

The optical coupling has been implemented as described in Section 2.3.3. In the presence of optical coupling, overall higher electrical outputs are observed for the colored PV module, suggesting that a higher fraction of both incident and fluorescence photons reaches the underlying PV cell. This is attributed to

the elimination of the air gap typically present between the fluorescent film and the cell when not optically coupled, meaning the elimination of the PMMA–air and air–Si interfaces. Therefore, an higher fraction of incident light is transmitted through the film to the PV cell. In addition, some of the emitted light trapped in the film can then reach the cell surface by travelling through the optical coupling medium, which possesses

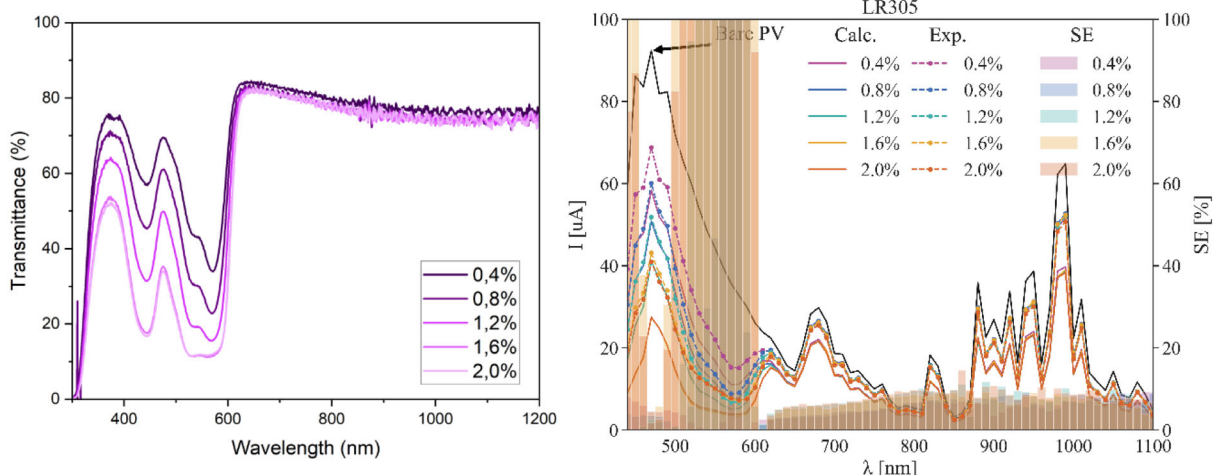


Figure 10. Result of the measured (exp.) and the simulated (calc.) SR in current of the analyzed system integrating LR305 film (on the left). The chart also reports the calculated spectral SE in percentage (SE%) of the simulated PV devices response. The measured spectral transmittance $\tau(\lambda)$ of the filters at different concentrations is reported in the chart on the right.

Table 3. Measured and simulated short-circuit currents of the devices, relative percentage SE of the I_{SC} of the analyzed DUT integrating the fluorescent films without optical coupling.

wt	DQ-TH2			LR305		
	I_{SC} calc. [mA]	I_{SC} exp. [mA]	SE%	I_{SC} calc. [mA]	I_{SC} exp. [mA]	SE%
0.40%	11.09	13.98	4.3%	11.22	13.93	3.8%
0.80%	10.25	12.73	3.8%	10.06	12.66	4.2%
1.20%	9.43	12.6	6.3%	8.94	11.62	5.3%
1.60%	8.77	11.06	4.3%	7.78	11.05	8.7%
2.00%	12.38	15.27	3.6%	7.78	10.70	7.4%

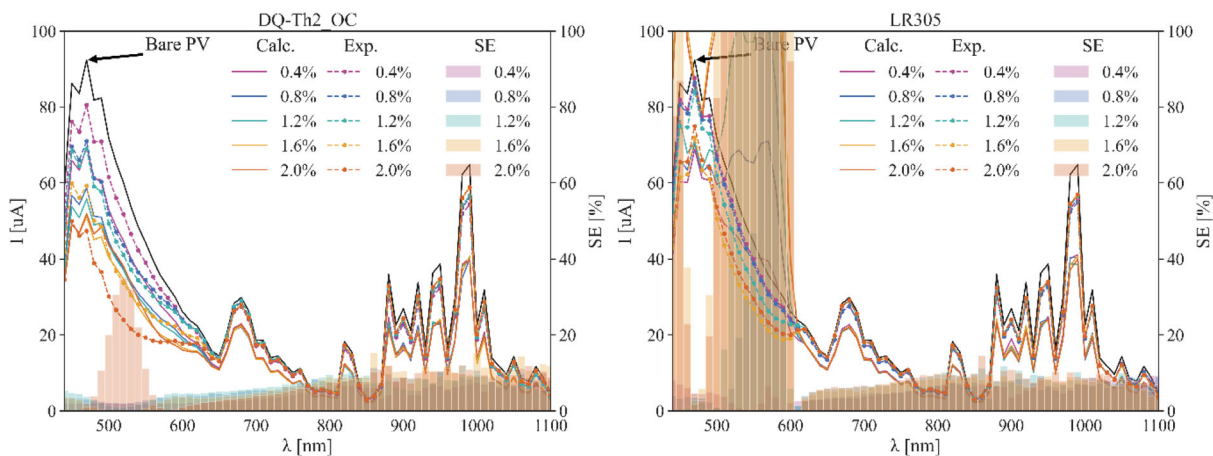


Figure 11. Result of the measured (exp.) and the simulated (calc.) SR in current of the analyzed system integrating DQ-Th2 film (on the left) and LR305 film (on the right) with optical coupling. The chart also reports the calculated spectral SE in percentage (SE%) of the simulated PV devices response.

a refractive index similar to that of PMMA. The trend of SRs with increasing dye concentration is still replicated by the simulations (Figure 11).

Predictions of the integrated I_{SC} show generally lower SE% values with respect to data, except for LR305 1.6% and 2.0% samples. The higher resulting SE% is attributed to dye aggregation

Table 4. Measured and simulated short-circuit currents of the devices, relative percentage SE of the I_{SC} of the analyzed DUT integrating the fluorescent films with optical coupling.

wt	DQ-TH2 with OC			LR305 with OC		
	I_{SC} calc. [mA]	I_{SC} exp. [mA]	SE%	I_{SC} calc. [mA]	I_{SC} exp. [mA]	SE%
0.40%	13.83	16.82	3.2%	14.29	17.52	3.4%
0.80%	12.57	16.06	4.7%	16.48	17.25	0.2%
1.20%	12.34	15.87	4.9%	19.26	16.83	2.1%
1.60%	11.71	14.75	4.3%	27.71	15.35	64.8%
2.00%	11.99	13.28	1.0%	26.10	15.82	42.2%

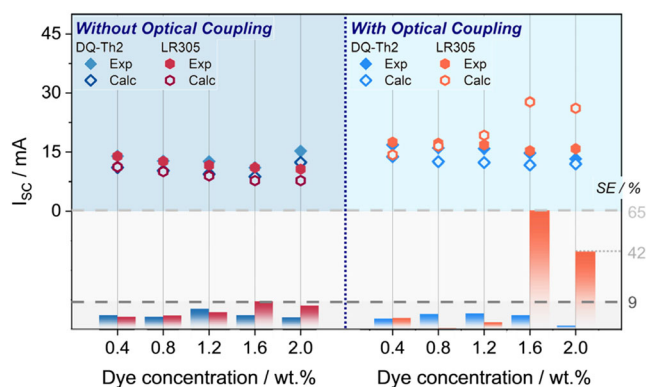


Figure 12. Experimental and calculated I_{SC} values for the DQ-Th2 and LR305 series, before (left) and after (right) introducing the optical coupling. The SE% for each pair of exp.–calc. values is displayed as a column plot, with notable marks displayed on the furthest right axis.

phenomena occurring during the preparation of the films at higher dye concentration and to the enhanced effect of film fluorescence due to optical coupling, which has not yet been considered at this stage of model development (Table 4 and Figure 12).

3.3.2. Colorimetric Characterization and I_{SC} Reduction Compared to the Bare Cell

The ability of the film to change the aesthetic appearance of the bare PV was evaluated via colorimetric tests on the samples, by using a colorimeter, with and without optical coupling. The evaluation was performed by calculating the difference in color (ΔE_{00}) between the bare PV and the samples. Preliminary results highlight that the samples of the series LR305, optically coupled with the bare cell, show stronger differences on the perceived color and smaller reduction in the short-circuit current of the final laminate, compared to the optically coupled DUT of the DQ-Th2 series (Figure 13). In particular, the DUTs integrating the DQ-Th2 films show a lower difference in color when compared to the bare PV cell, with main differences relying in the modification of the hues toward the red region, a slight modification of the chroma and the shift of the lightness toward lower values. A more pronounced shift of the hues toward the red region, along with a significant increase in chroma, can be observed. When including the optical coupling effect, the lightness of the DUTs decreases for both DQ-Th2 and LR305 series, most likely due to the reduced total reflectance. The representation of the DUTs color in the CIELab color space can be found in Figure 14.

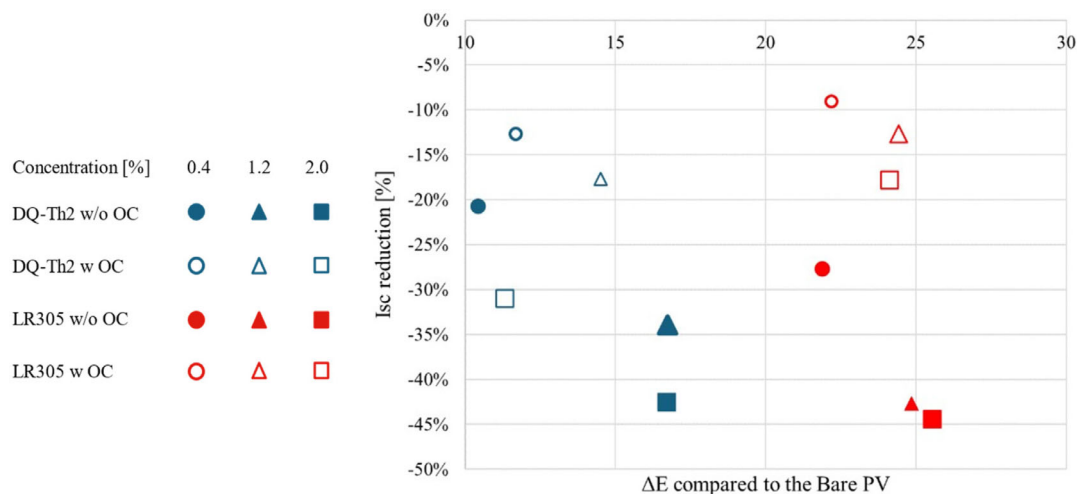


Figure 13. Colorimetric characterization (color difference) and I_{SC} reduction of the DUT with the fluorescent polymeric films, with (w) and without (w/o) optical coupling, compared to the bare PV cell.

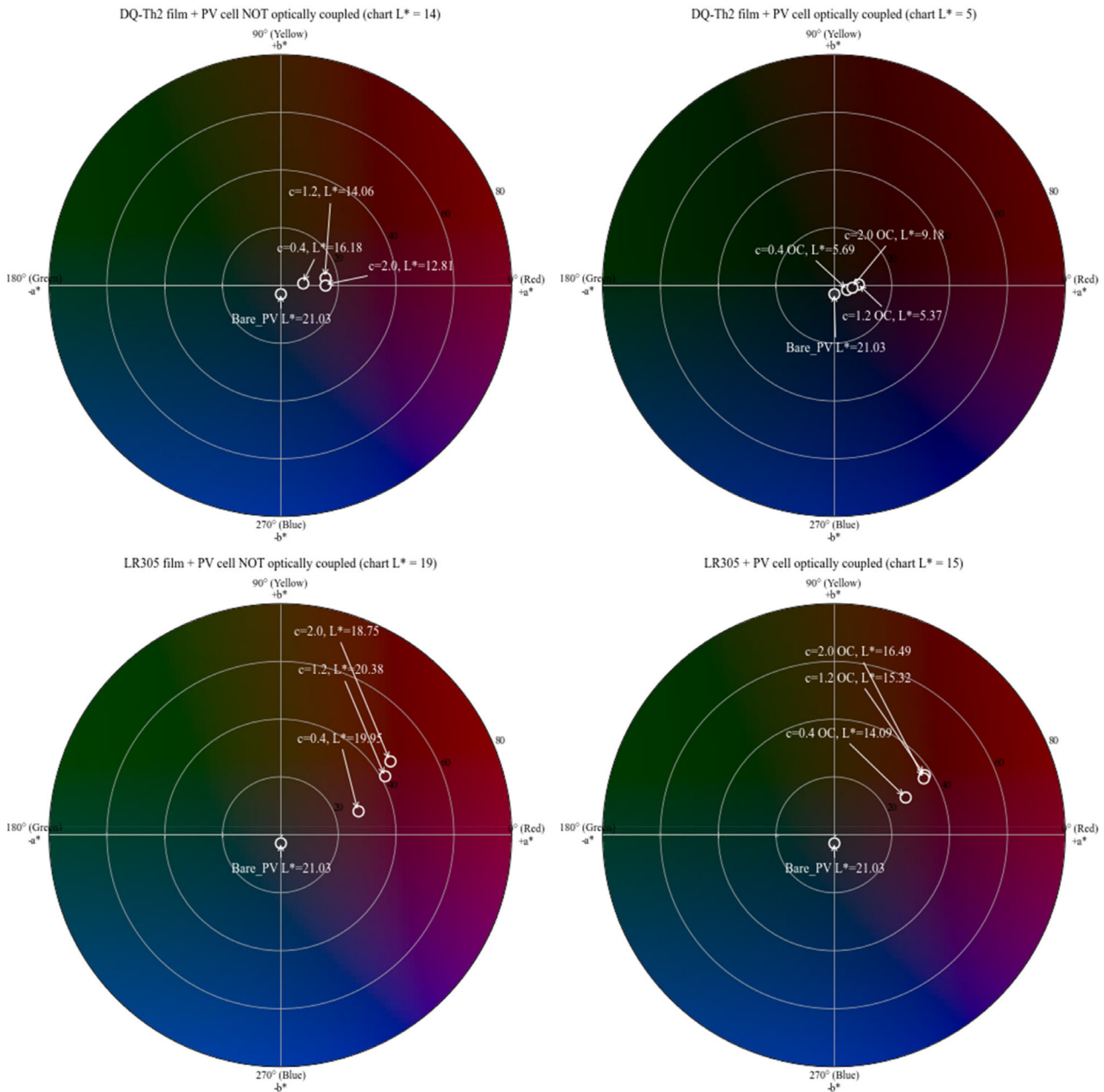


Figure 14. Representation of the DUT integrating the colored fluorescent films under investigation, in the CIE Lab color space. The DUTs are plotted in configurations both with and without optical coupling. To account for differences in color lightness (L^*), samples with similar lightness levels have been plotted on a dedicated chart, where the color background provides a reference lightness for each group.

4. Conclusions

This study presents a modeling framework for predicting the electrical performance of colored PV modules. The model demonstrates high accuracy across a range of coloring technologies, including selective absorbers, diffusive layers, and fluorescent films. For colored filters and diffusive glass, the model achieved SEs below 1% for short-circuit current predictions and less than 2% for spectrally resolved responses. Even for more complex fluorescent polymeric films, where re-emission processes come

into play, the model maintained good reliability with low SEs on I_{SC} predictions. The ability to accurately predict PV module performance based on the optical properties of colored layers represents a significant step forward in the development of aesthetically pleasing BIPV. This predictive capability can substantially reduce the time and resources required for prototype development, allowing for rapid optimization of both aesthetic appeal and energy generation efficiency. Furthermore, the model's versatility in handling different coloring mechanisms provides valuable insights into the trade-offs between visual appearance and

electrical performance. As the demand for BIPV solutions continues to grow, this modeling approach offers a powerful tool for designers and manufacturers to create visually attractive solar modules without compromising on power output. Future work could focus on extending the model to larger scale systems and incorporating additional factors such as optical coupling among module's stack components, temperature effects and long-term durability, as well as implementing the possibility to reliably predict through modeling the color of the final laminated module.

5. Experimental Section

Materials: The optical filters used as absorptive colored layers are a series of squared $50 \times 50 \times 3$ mm³ longpass and bandpass filters (Melles Griot) made from different colors of Schott glass (longpass: OG590, RG695; bandpass: BG18, KG1, VG9). The optical diffusers used as scattering white layers are a series of round (diameter 50 mm, thickness 2 mm) ground glass diffusers made of N-BK7 glass. They possess one polished side and one sandblasted side, available with four different grits: Thorlabs DG20-120, DG20-220, DG20-600, DG20-1500.

A low autofluorescence microscopy immersion oil with refractive index of 1.518 (Thorlabs OILCL30) was employed for the optical coupling between PV cell and colored layers.

Optical and Electrical Characterizations: Transmittance ($T(\lambda)$) of the colored filters and diffusers was collected on a CARY5000 double-beam spectrophotometer, equipped with a poly(tetrafluoroethylene)-coated integration sphere and with a spectral bandwidth of 2 nm.

Transmittance ($T(\lambda)$) and reflectance ($R(\lambda)$) of fluorescent films were collected on a Shimadzu UV-2600 spectrometer, equipped with an integration sphere and with a spectral bandwidth of 1 nm.

The colorimetric measures were performed by using a vertical spectrophotometer 3color SV-300 (wavelength range 400–700 nm, D65 illuminant and CIE 10° standard observer).

A Horiba JobinYvon Fluorolog-3 spectrofluorometer equipped with double-grating monochromators on the excitation side and iHR320 spectrograph on the emission side was used a light source. The excitation monochromator is equipped with two 1200 lines mm⁻¹ gratings blazed at 330 nm (2 nm mm⁻¹ dispersion). A spectral bandwidth of 6 nm was used for the experiments. A vis/NIR transmitting optical fiber (Thorlabs liquid lightguide LLG3-4Z, 5 mm diameter, 420–2000 nm) was used to direct the light from the Fluorolog-3 onto the PV cell. An uncoated UV fused silica plano-convex lens (Melles Griot 01LUP049, diameter 50 mm, 185–2100 nm) was used to collimate the beam. The optical power of the incident beam was measured through a Gentec-EO PowerMeter, model PRONTO-Si (technical specifications can be found in Table S2, Supporting Information). A monocrystalline, single-module Si PV cell (IXYS Corporation, series IXOLAR SolarBIT, model KXOB22-12X1F) with active area of 2.2×0.7 cm² has been chosen as test PV cell. I_{SC} SRs were measured with a Keithley 2450 Graphical Source Measure Unit (SMU, technical specifications can be found in Table S1, Supporting Information) synchronized with the Fluorolog-3. I_{SC} spectra were acquired between 440 and 1100 nm with a step of 10 nm.

Supporting Information

Supporting Information is available from the Wiley Online Library or from the author.

Acknowledgements

M.P. and I.M. contributed equally to this work. This study is a result of the research projects: “nuovi Concetti, mAteriali e tecnologie per l'iNtegrazione del fotoVOLTaico negli edifici in uno scenario di

generazione diffuSa' [CANVAS], funded by the Italian Ministry of the Environment and the Energy Security, through the Research Fund for the Italian Electrical System (type-A call, published on G.U.R.I. n. 192 on 18-08-2022) and “Network 4 Energy Sustainable Transition—NEST,” Spoke 1., Project code PE0000021, funded under the National Recovery and Resilience Plan (NRRP), Mission 4, Component 2, Investment 1.3—Call for tender No. 1561 of 11.10.2022 of Ministero dell'Università e della Ricerca (MUR); funded by the European Union—NextGenerationEU. Investimento 1.3—Avviso “Partenariati estesi alle università, ai centri di ricerca, alle aziende per il finanziamento di progetti di ricerca di base”—D.D. n. 341 del 15 marzo 2022—CUP: D53C22002590002.” The authors would like to thank Prof. Andrea Pucci (University of Pisa) and Dr. Giulio Goti (ICCOM-CNR) for their contribution in the preparation of fluorescent films.

Conflict of Interest

The authors declare no conflict of interest.

Author Contributions

Martina Pelle: Conceptualization (equal); Data curation (lead); Formal analysis (lead); Investigation (equal); Writing—original draft (lead). **Irene Motta:** Conceptualization (equal); Data curation (lead); Formal analysis (lead); Investigation (equal); Writing—original draft (equal). **Gabriella Gonnella:** Conceptualization (supporting); Data curation (supporting); Formal analysis (supporting); Investigation (equal); Writing—original draft (supporting). **Alessio Dessi:** Conceptualization (equal); Data curation (equal); Formal analysis (equal); Investigation (equal); Writing—original draft (equal). **Lidia Armelao:** Funding acquisition (equal); Supervision (equal). **Gregorio Bottaro:** Conceptualization (equal); Data curation (equal); Formal analysis (equal); Investigation (equal); Writing—original draft (equal). **Massimo Calamante:** Conceptualization (equal); Investigation (equal); Writing—original draft (equal); Writing—review & editing (equal). **Alessandro Mordini:** Funding acquisition (equal); Supervision (equal). **David Moser:** Funding acquisition (equal); Supervision (equal).

Data Availability Statement

The data that support the findings of this study are available from the corresponding author upon reasonable request.

Keywords

building-integrated photovoltaics, colored photovoltaics, integrated photovoltaics, predictive models

Received: August 3, 2024

Revised: October 28, 2024

Published online:

- [1] M. Victoria, N. Haegel, I. M. Peters, R. Sinton, A. Jäger-Waldau, C. Del Cañizo, C. Breyer, M. Stocks, A. Blakers, I. Kaizuka, K. Komoto, A. Smets, *Joule* **2021**, 5, P1041.
- [2] N. M. Haegel, R. Margolis, T. Buonassisi, D. Feldman, A. Froitzheim, R. Garabedian, M. Green, S. Glunz, H.-M. Henning, B. Holder, I. Kaizuka, B. Kroposki, K. Matsubara, S. Niki, K. Sakurai, R. A. Schindler, W. Tumas, E. R. Weber, G. Wilson, M. Woodhouse, S. Kurtz, *Science* **2017**, 356, 141.

- [3] B. J. Stanbery, M. Woodhouse, J. Van De Lagemaat, *Sol. RRL* **2023**, *7*, 2300102.
- [4] C. Wilson, A. Grubler, N. Bento, S. Healey, S. De Stercke, C. Zimm, *Science* **2020**, *368*, 36.
- [5] F. Creutzig, J. Hilaire, G. Nemet, F. Müller-Hansen, J. C. Minx, *Energy Res. Soc. Sci.* **2023**, *105*, 103276.
- [6] A. Scognamiglio, A. Berni, F. Frontini, C. S. Polo López, L. Maturi, in *27th European Photovoltaic Solar Energy Conf. and Exhibition*, Frankfurt, September **2012**, <https://doi.org/10.4229/27thEUPVSEC2012-5BV.1.1>.
- [7] J. Escarre, H.-Y. Li, L. Sansonnens, F. Galliano, G. Cattaneo, P. Heinsteinst, S. Nicolay, J. Bailat, S. Eberhard, C. Ballif, L.-E. Perret-Aebi, in *2015 IEEE 42nd Photovoltaic Specialist Conf.*, New Orleans, June **2015**, <https://doi.org/10.1109/PVSC.2015.7355630>.
- [8] M. Pelle, E. Lucchi, L. Maturi, A. Astigarraga, F. Causone, *Energies* **2020**, *13*, 4506.
- [9] <https://www.bipvmeetshistory.eu/en-gb/>.
- [10] E. Lucchi, I. Dall'orto, A. Peluchetti, L. Toledo, M. Pelle, C. Polo López, G. Guazzi, *Energy Policy* **2022**, *161*, 112772.
- [11] B. Petter Jelle, C. Breivik, H. Drolsum Rokenes, *Sol. Energy Mater. Sol. Cells* **2012**, *100*, 69.
- [12] M. Pelle, E. Canosci, G. Luzi, L. Maturi, in *Inter. Conf. on Solar Energy for Buildings and Industry*, Kassel, September **2022**.
- [13] L. O. Grobe, M. Terwilliger, S. Wittkopf, *Proc. ATI 2020: Smart Buildings, Smart Cities*, Izmir, April **2020**, <https://doi.org/10.5281/ZENODO.4049446>.
- [14] T. E. Kuhn, C. Erban, M. Heinrich, J. Eisenlohr, F. Ensslen, D. H. Neuhaus, *Energy Build.* **2021**, *231*, 110381.
- [15] A. Borja Block, J. Escarre Palou, M. Courtant, A. Virtuani, G. Cattaneo, M. Roten, H.-Y. Li, M. Despeisse, A. Hessler-Wyser, U. Desai, A. Faes, C. Ballif, *Energy Build.* **2024**, *314*, 114253.
- [16] T. Gewohn, M. R. Vogt, B. Lim, C. Schinke, R. Brendel, *IEEE J. Photovolt.* **2021**, *11*, 138.
- [17] M. H. Saw, J. P. Singh, Y. Wang, K. E. Birgersson, Y. S. Khoo, *IEEE J. Photovolt.* **2020**, *10*, 1027.
- [18] T. Masuda, Y. Kudo, D. Banerjee, *Coatings* **2018**, *8*, 282.
- [19] G. Peharz, K. Berger, B. Kubicek, M. Aichinger, M. Grobbauer, J. Gratzner, W. Nemitz, B. Großschädl, C. Auer, C. Prietl, W. Waldhauser, G. C. Eder, *Renewable Energy* **2017**, *109*, 542.
- [20] P. Shen, G. Wang, B. Kang, W. Guo, L. Shen, *ACS Appl. Mater. Interfaces* **2018**, *10*, 6513.
- [21] B. Blasi, T. Kroyer, T. Kuhn, O. Hohn, *IEEE J. Photovolt.* **2021**, *11*, 1305.
- [22] J. C. Ortiz Lizcano, S. Villa, Y. Zhou, G. Frantzi, K. Vattis, A. Calcabrini, G. Yang, M. Zeman, O. Isabella, *Sol. RRL* **2023**, *7*, 2300256.
- [23] J. C. Ortiz Lizcano, P. Procel, A. Calcabrini, G. Yang, A. Ingenito, R. Santbergen, M. Zeman, O. Isabella, *Prog. Photovolt.: Res. Appl.* **2022**, *30*, 401.
- [24] A. Røyset, T. Kolås, B. P. Jelle, *Energy Build.* **2020**, *208*, 109623.
- [25] G. Peharz, A. Ulm, *Renewable Energy* **2018**, *129*, 299.
- [26] T. Gewohn, C. Schinke, B. Lim, R. Brendel, *AIP Adv.* **2021**, *11*, 095104.
- [27] L. H. Slooff-Hoek, A. R. (Teun) Burgers, A. J. Carr, T. Minderhoud, G. Gijzen, T. Sepers, W. van Strien, in *8th World Conf. on Photovoltaic Energy Conversion*, Milan, September **2022**, <https://doi.org/10.4229/WCPEC-82022-3BO.14.3>.
- [28] M. Pelle, F. Causone, L. Maturi, D. Moser, *Energies* **2023**, *16*, 1991.
- [29] N. K. Kalluvettukuzhy, M. R. Maciejczyk, I. Underwood, N. Robertson, *J. Mater. Chem. A* **2023**, *11*, 13195.
- [30] E. Klampaftis, D. Ross, K. R. McIntosh, B. S. Richards, *Sol. Energy Mater. Sol. Cells* **2009**, *93*, 1182.
- [31] I. Motta, G. Bottaro, M. Rando, M. Rancan, R. Seraglia, L. Armelao, *J. Mater. Chem. A* **2024**, *12*, 22516.
- [32] E. C. Carter, J. D. Schanda, R. Hirschler, S. Jost, M. R. Luo, M. Melgosa, Y. Ohno, M. R. Pointer, D. C. Rich, F. Viénot, L. Whitehead, J. H. Wold, *CIE 015:2018 Colorimetry*, 4th ed., International Commission on Illumination (CIE). <https://doi.org/10.25039/tr.015.2018>.
- [33] C. Papucci, T. A. Geervliet, D. Franchi, O. Bettucci, A. Mordini, G. Reginato, F. Picchioni, A. Pucci, M. Calamante, L. Zani, *Eur. J. Org. Chem.* **2018**, *2018*, 2657.
- [34] G. Goti, G. Reginato, C. Coppola, A. Dessì, D. Franchi, A. Mordini, A. Picchi, A. Pucci, A. Sinicropi, L. Zani, M. Calamante, *Eur. J. Org. Chem.* **2024**, *27*, e202482401.
- [35] C. Papucci, R. Charaf, C. Coppola, A. Sinicropi, M. Di Donato, M. Taddei, P. Foggi, A. Battisti, B. De Jong, L. Zani, A. Mordini, A. Pucci, M. Calamante, G. Reginato, *J. Mater. Chem. C* **2021**, *9*, 15608.
- [36] P. Della Sala, N. Buccheri, A. Sanzone, M. Sassi, P. Neri, C. Talotta, A. Rocco, V. Pinchetti, L. Beverina, S. Brovelli, C. Gaeta, *Chem. Commun.* **2019**, *55*, 3160.